NUCLEAR INSTRUMENTS AND METHODS 109 (1973) 3–11; © NORTH-HOLLAND PUBLISHING CO.

LINE SHAPES OF DOPPLER SHIFTED γ-RAYS FROM COINCIDENCE AND SINGLES SPECTRA IN MEASUREMENTS OF NUCLEAR LIFETIMES

E. J. HOFFMAN and D. M. VAN PATTER

*Bartol Research Foundation of the Franklin Institute, Swarthmore, Pennsylvania 19081, U.S.A.**

D. G. SARANTITES and J. H. BARKER

Department of Chemistry, Washington University, St. Louis, Missouri 63130, U.S.A.†

Received 17 January 1973

A procedure is described for extracting nuclear lifetimes from the analysis of line shapes of γ-rays from either coincidence or singles spectra obtained from Doppler-shift attenuation experiments. The nuclear and electronic stopping powers in a given slowing down medium are independently adjusted to give the line shape and lifetimes of "standard" Doppler-shifted γ-rays, the lifetimes of which have been determined by other independent methods. The stopping power thus calibrated is then used to determine the lifetimes of other transitions from Doppler-shift attenuation experiments in the same stopping medium. Line shapes are obtained by including the effects (a) of the recoils that escape the target, (b) of the decay of other levels into the state in question, (c) of the γ- or particle-detection angles and their corresponding solid angles, (d) of the integration over the distribution of recoils in the singles experiments including angular correlation effects to a good approximation for angles of observation $\leq 30°$ to the beam direction, and (e) of the detector response assumed to be gaussian. Lifetimes are obtained from comparison with experiment using both a line shape fitting technique and the $F(\tau)$ or centroid-shift technique.

1. Introduction

The Doppler-shift attenuation (DSA) technique has been used in recent years by many investigators (see for example refs. 1–6) for obtaining nuclear level lifetimes in the region 10^{-14}–10^{-11} s. The most common version of this technique assumes that an excited state is populated by a nuclear reaction which proceeds in a very short time ($\ll 10^{-14}$ s). The state then decays by γ-ray emission at a later measurable time. The shift in energy of the γ-ray emitted from the nucleus recoiling in matter depends on the velocity of the nucleus at the time of emission. The collection of nuclei which slow down in a given medium will then give a spectrum of shifts the details of which depend on the slowing-down process and the lifetime of the state involved. Under suitable conditions lifetimes can be extracted if the slowing-down process can be adequately calculated. In general the nuclear reactions that can be used to populate the nuclear states must either be near threshold in singles measurements or carried out in coincidence with sufficient energy selection to limit the observation to states with primarily direct population. This usually limits the bombarding energy to low values and yields recoil velocities $< 1\%$ of the velocity of light, depending on the mass of the projectile and of the recoiling nucleus. Under such conditions the moving recoils lose energy at high initial velocities primarily via collisions with electrons [collisions with nuclei can be neglected[7]], and at lower velocities via collisions with atoms.

2. Formalism for the DSA method

2.1. The line-shape method

The energy shift of a γ-ray emitted in the direction $\boldsymbol{n}_{\mathrm{d}}$ from an ensemble of nuclei moving with velocity $\boldsymbol{v}(t)/c = \boldsymbol{\beta}(t)$ is to first order in β

$$\Delta E_\gamma = E_\gamma^0\, \boldsymbol{\beta}(\theta_{\mathrm{R}} t) \cdot \boldsymbol{n}_{\mathrm{d}} = E_\gamma^0\, \beta(\theta_{\mathrm{R}} t) \cos \Theta_{\mathrm{d}} . \quad (1)$$

If the recoiling nuclei are initially emitted in the direction defined by θ_{R}, ϕ_{R} as in fig. 1, then at the time of decay t the recoils are moving on an average cone defined by $\theta_{\mathrm{c}}(t)$ and ϕ_{c} about the original recoil direction due to the slowing-down collisions. In this case $\cos \Theta_{\mathrm{d}}$ is given by

$$\cos \Theta_{\mathrm{d}} = \cos \theta_{\mathrm{c}}(t) \cos \Theta_{\mathrm{R}} + \sin \theta_{\mathrm{c}}(t) \sin \phi_{\mathrm{c}} \sin \Theta_{\mathrm{R}} , \quad (2)$$

$$\cos \Theta_{\mathrm{R}} = \cos \theta_{\mathrm{R}} \cos \theta_{\mathrm{d}} + \sin \theta_{\mathrm{R}} \sin \phi_{\mathrm{R}} \sin \theta_{\mathrm{d}} . \quad (3)$$

The fraction of reactions that lead to decay via the state of interest between t and $t + \mathrm{d}t$ and give an energy shift ΔE_γ of eq. (1) is given by

* Work supported in part by the National Science Foundation.
† Work supported in part by the U.S. Atomic Energy Commission under Contract No. AT(11-1)-1530 and AT(11-1)-1760.

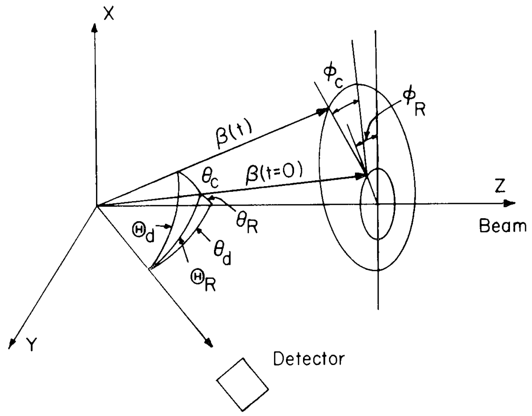

Fig. 1. Schematic representation of the geometry involved in a DSA measurement. The recoil cone about the beam axis z is defined by the angles θ_R and ϕ_R with a velocity vector $\beta(t=0)$ indicated. The collision cone with $\beta(t=0)$ as axis is defined by the angles $\theta_c(t)$ and $\phi_c(t)$. The detection angle relative to the beam direction is θ_d.

$$\frac{dN(\Delta E_\gamma)}{N^0} = R(t)\,dt\,\frac{d\sigma(\theta_R)}{d\Omega}\,d\Omega\,d\phi_R\,W(\theta_R\phi_R\theta_d), \quad (4)$$

where

$$R(t) = \frac{1}{\tau_1}\left\{f_1^0 \exp(-t/\tau_1) + \sum_{i=2}^{n} f_i^0 \frac{\tau_1}{\tau_i-\tau_1}\left[\exp(-t/\tau_i) - \exp(-t/\tau_1)\right]\right\} \quad (5)$$

is the fraction of nuclei that decay per unit time through the state of interest at time t; $d\sigma(\theta_R)/d\Omega$ is the relative differential cross-section for the initial emission of recoils at an angle θ_R, which for reactions proceeding via formation and decay of a compound nucleus can be written as

$$\frac{d\sigma(\theta_R)}{d\Omega} = 1 + A_2 P_2(\cos\theta_{CM}) + A_4 P_4(\cos\theta_{CM}), \quad (6)$$

where θ_{CM} is the center of mass angle for the emission of the light particle; and

$$W(\theta_R\phi_R\theta_d) = 1 + A_2(\theta_R\phi_R)\,P_2(\cos\theta_d) + A_4(\theta_R\phi_R)\,P_4(\cos\theta_d) \quad (7)$$

is the angular correlation function for the emission of a γ-ray at an angle θ_d to the beam when the initial recoil was emitted in the direction (θ_R, ϕ_R).

The line spectrum is then obtained via eqs. (4) and (1) by allowing t, θ_R and ϕ_R to take all their possible values. Clearly at some time t_r the recoils come essentially to rest and a fraction

$$\frac{dN(\Delta E_\gamma=0)}{N^0} = P(t_r)\,\frac{d\sigma(\theta_R)}{d\Omega}\,d\Omega\cdot W(\theta_R\phi_R\theta_d)\,d\phi_R \quad (8)$$

of reactions contributes zero shift to the line spectrum. In eq. (8)

$$P(t_r) = \sum_{i=1}^{n} f_i^0 \exp(-t_r/\tau_i) + \sum_{i=2}^{n} f_i^0 \frac{\tau_1}{\tau_i-\tau_1}\left[\exp(-t_r/\tau_i) - \exp(-t_r/\tau_1)\right]$$

is the fraction of nuclei that have not yet decayed through the state of interest. The assumed decay scheme is shown in fig. 2, where $f_1^0 = N_1^0/N^0$ is the fraction of reactions that populate promptly the observed state and $f_i^0 = N_i^0/N^0$ for $i > 1$ are the fractions for population of the observed state by a single decay via levels with lifetimes τ_i.

Since the probability term of eq. (4) is independent of the collision angle ϕ_c, eq. (1) can be averaged over ϕ_c to yield for the shift

$$\Delta E = E_\gamma^0\,\beta(\theta_R t)\cos\theta_c(t)\times(\cos\theta_R\cos\theta_d + \sin\theta_R\sin\theta_d\sin\phi_R). \quad (9)$$

Of particular interest in lifetime measurements by the DSA method are either coincidence experiments in which the light particle is detected at some angle, preferably near 180° to the beam, or singles experiments carried out near the reaction threshold. In these two cases the reaction kinematics define the initial recoil cone to narrow limits (half angles $\leq 6°$ on the average). Furthermore, for $\theta_d = 0°$ the angular correlation function of eq. (7) becomes independent of ϕ_R. As the detection angle is increased from 0° to 90° the dependence of $W(\theta_R\phi_R\theta_d)$ on ϕ_R becomes progressively more important. However, for small detection angles ($\theta_d \leqslant 30°$) the correlation function may be assumed

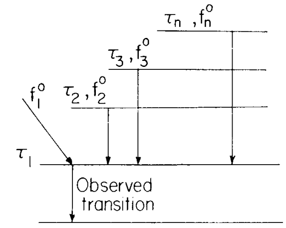

Fig. 2. Partial decay scheme showing the genetic relationships that have been incorporated in the present analysis of DSA data. The fractions $f_i^0 = N_i^0/\sum_i N_i^0$ represent the fraction of reactions that proceed via the indicated path.

independent of ϕ_R. For $\theta_R = 0°$ which corresponds to the emission of the light particle at $\theta_L = 0°$ or 180° the correlation for a given transition $J_1 \to J_2$ with known multipole mixing ratio is in principle known[8]) and exhibits the largest anisotropy. For $\theta_L = 90°$ the resulting correlation has its smallest anisotropy. The singles correlation about the beam direction on the other hand corresponds to the average correlation for all θ_L values. Since the singles correlation can be measured for most cases in the same experiment, a reasonable approximation to the correlation may be obtained by assuming a simple linear dependence of $A_K(\theta_R)$ on θ_L for $0 \leq \theta_L \leq \frac{1}{2}\pi$, namely

$$A_K(\theta_R) = A_K^0 + \frac{4}{\pi}(\bar{A}_K - A_K^0)\,\theta_L. \qquad (10)$$

As it will be shown, however, the effect on the line shape of $d\sigma(\theta_R)/d\Omega$ with θ_L is more important than the angular correlation term $W(\theta_R, \theta_d)$ at least for $\theta_d \leq 30°$.

In order to evaluate $\beta(\theta_R t)$, the stopping power theory of Lindhard, Scharff and Schiott[7]) (LSS) as modified by Blaugrund[2]) was employed with the stopping power taken as

$$\frac{d\varepsilon}{d\rho} = f_e\left(\frac{d\varepsilon}{d\rho}\right)_e + f_n\left(\frac{d\varepsilon}{d\rho}\right)_n, \qquad (11)$$

where

$$\left(\frac{d\varepsilon}{d\rho}\right)_e = k\varepsilon^{\frac{1}{2}}, \qquad (12)$$

and

$$\left(\frac{d\varepsilon}{d\rho}\right)_n = \frac{\varepsilon^{\frac{1}{2}}}{0.67+2.07\,\varepsilon+0.03\,\varepsilon^2} \qquad (13)$$

are the electronic and nuclear stopping powers, respectively. The quantities ε and ρ are the (LSS) dimensionless parameters for energy and length. For $1 < \varepsilon < 20$, eq. (13) was approximated[2]) by $(d\varepsilon/d\rho)_n = 0.4\varepsilon^{-\frac{1}{2}}$. The factors f_e and f_n have been introduced to adjust the two stopping powers relative to the values of the (LSS) theory to fit the line shapes and lifetimes of "standard" γ-rays with lifetimes measured by different techniques. The $\cos\theta_c(t)$ in eqs. (2) and (9) is the average collision cosine of Blaugrund[2]).

2.2. THE CENTROID-SHIFT METHOD

In this method the centroid shift for γ-rays emitted from an ensemble of nuclei moving with velocity $\boldsymbol{\beta}(t)$ is

$$\langle \Delta E_\gamma \rangle = \bar{E}_\gamma - E_\gamma^0 = E_\gamma^0\,\bar{\beta}(0)\,F(\tau_1, \tau_2, \ldots)\cos\theta_d, \qquad (14)$$

where $F(\tau_1, \tau_2, \ldots)$ is the ratio of the observed shift divided by the maximum shift that would occur if all nuclei decayed at $t = 0$. Thus, $\langle \Delta E_\gamma \rangle$ is obtained from eqs. (4) and (9) by integrating over time from 0 to ∞ to give for $F(\tau_1, \tau_2, \ldots)$

$$F(\tau_1, \tau_2, \ldots) = \frac{1}{\bar{\beta}(0)}\int_0^\infty R(t)\cos\theta_c(t)\,\bar{\beta}(t)\,dt, \qquad (15)$$

where the integrations over ϕ_R and ϕ_c have been carried out and

$$\bar{\beta}(t) = \int_{\theta_R} d\Omega\,\frac{d\sigma(\theta_R)}{d\Omega}\,W(\theta_R\theta_d)\,\beta(\theta_R t)\cos\theta_R. \qquad (16)$$

Furthermore, for a coincidence measurement (one value of θ_R) or a singles measurement very near the threshold ($\theta_R = 0°$) eq. (15) becomes

$$F(\tau_1,\tau_2,\ldots) = \frac{\cos\theta_R}{\beta(\theta_R, t=0)}\int_0^\infty R(t)\,\beta(\theta_R t)\cos\theta_c(t)dt. \qquad (17)$$

It can be shown that $F(\tau_1, \tau_2, \ldots)$ in eq. (15) which applies to singles measurements at any angle θ_d of detection relative to the beam direction is to good approximation independent of θ_d. This is also verified experimentally. Therefore, from the slope of a plot of the centroid shift vs $\cos\theta_d$ (see eq. 14) one can determine $F(\tau_1, \tau_2, \ldots)$. In turn the lifetime τ_1 can be obtained from a plot of $F(\tau_1, \tau_2, \ldots)$ vs τ_1 with $F(\tau_1, \tau_2, \ldots)$ evaluated via eqs. (15) or (17). Alternatively, using eq. (5) one obtains for the scheme of fig. 2

$$F(\tau_1, \tau_2, \ldots, \tau_n) = \left(f_1^0 + \sum_{i=2}^n f_i^0\,\frac{\tau_1}{\tau_1 - \tau_i}\right)F(\tau_1) + \sum_{i=2}^n f_i^0\,\frac{\tau_i}{\tau_i - \tau_1}\,F(\tau_i), \qquad (18)$$

where $F(\tau_i)$ is obtained from (15) or (17) with $R(t) = (1/\tau_i)\exp(-t/\tau_i)$. From eq. (18) one obtains $F(\tau_i)$ and consequently τ_i if the lifetimes and branching fractions for all levels involved are known.

3. Experimental procedures

In this work we have selected Ni as the stopping medium and used the reactions $^{58,60}Ni(\alpha, p\gamma)^{61,63}Cu$ to test the assumptions of the DSA method both for singles and coincidence experiments. The $^4He^{++}$ beams employed varied in energy between 10.0–12.3 MeV, and were obtained either from the University of Pennsylvania Tandem Van de Graaff accelerator or the Washington University cyclotron.

3.1. Detection equipment and methods of counting

3.1.1. *Coincidence measurements*

For coincidence measurements miniature scattering chambers were employed that permitted annular Si surface barrier charged-particle detectors to be used with large volume Ge(Li) γ-ray detectors placed as close as 2.5 cm to the target for angles 0°–90° to the beam direction. The chambers were made of aluminium and were lined with 0.25 mm of tantalum or lead in which the beam was stopped. In some cases 0.4 cm Pb and 0.2 cm Cd was placed in front of the Ge(Li) detector to attenuate the low energy γ-rays. The annular detectors employed had an active area of 200 mm^2 and thickness of 0.5 or 1.0 mm. These were cooled either with a thermoelectric cooler or by a cold finger to -67 °C which decreased the leakage current by a factor of ≈ 100 and greatly improved detector stability. In these experiments the detectors subtended angles from 150°–170°, and were covered with 20 mg/cm^2 aluminium foil sufficient to stop the backscattered $^4He^{++}$ while allowing the transmission of the reaction protons.

Two Ge(Li) detectors (33 cm^3 and 35 cm^3) were employed which had actual resolutions of 4.0 and 2.2 keV fwhm at 1332 keV measured at the end of each experiment. Calibration peaks were introduced in the p–γ coincidence spectra by requiring coincidences between the Ge(Li) detector and a 5.08 cm × 5.08 cm NaI(Tl) detector which was shielded from the target but viewed a ^{207}Bi source that was also visible to the Ge(Li) detector. In this work the Ge(Li) crystals were located at 4.4 cm from the target.

The targets were isotopically enriched to 99.95% in ^{58}Ni and 99.1% in ^{60}Ni and consisted of 2.0 and 3.8 mg/cm^2 foils prepared by rolling of the metals. For some of the experiments 2 mg/cm^2 of Au was evaporated on the back side of the target in order to prevent the recoils from decaying in flight in the vacuum.

For data collection a 4096-channel pulse height analyzer was used which was interfaced to a PDP 8/L computer that had a buffer tape with 24 bit related address capability.

3.1.2. *Singles measurements*

The singles experiments were performed using the same scattering chambers. For γ-ray counting the Ge(Li) detectors were employed in anti-Compton arrangements which have been described elsewhere[9,10]. These anti-Compton spectrometers with their shieldings were located on angular correlation tables that permitted spectra to be taken between 0° and 110° to the beam direction.

3.2. Extraction of lifetimes

The mean lifetimes for several transitions were extracted from the γ-ray spectra employing both the line-shape and the centroid shift methods described in sect. 2. It is believed that the application of the line-shape method is essential in the extraction of lifetimes particularly for singles measurements and for transitions that show large shifts. When the experimental shapes are well reproduced by the calculation then the two methods should give results free of systematic errors. In this work a FORTRAN IV computer code called SHAPES was written which permitted the calculation of line shapes from the parametric eqs. (4) and (9). For each shape the corresponding $F(\tau)$ was also obtained. In this calculation for singles spectra decay from up to four higher lying states could be included. However, it is recommended that only states with $0.7 < f_1^0 \leq 1.0$ be analyzed. The obtained line shapes are normalized to the area of the experimental data and a search for minimum χ^2 is made by allowing the level lifetime to vary. In the present experiments even when a rather thick target of ^{58,60}Ni was used, a small fraction of the recoils escaped the target. The line spectrum from these escaping recoils is quite different from that of the recoils that stop in the target and it must be properly evaluated. This was approximated by dividing the range in ten parts and calculating for each the spectrum from the fraction that decays in the target and the fraction that escapes and contributes a full shift at the proper reduced velocity. This effect is important and if neglected may result in lifetimes which are too short by as much as 20% for targets thick enough to stop 90% of the recoils.

4. Results and discussion

4.1. Calibration of the stopping power in Ni

Usually the largest uncertainty in the measurement of lifetimes via the DSA method arises from uncertainties in the stopping power of the recoiling ions in many stopping materials. These uncertainties can be substantially reduced if the stopping power of a particular ion in a medium is empirically adjusted to reproduce the line shapes and lifetimes of several transitions with known lifetimes from different measurements that do not involve the slowing down process.

In this work we have employed the 669.7 and

1546.8 keV transitions in ^{63}Cu with mean lifetimes[11,12]) of 310±30 and 203+20 fs, respectively. We have measured the Doppler shift of these transitions in a coincidence experiment employing the reaction ^{60}Ni(α,pγ) ^{63}Cu. For the 669.7 keV transition, only a centroid shift was obtained. The line shape of the 1546.8 keV γ-ray was then fitted in a series of calculations in which τ was kept at 203 fs, and f_e and f_n of eq. (11) were varied. Fig. 3 shows the χ^2 as a function of f_e for four cases: (a) $f_n = 1.0$ with f_e varying (dashed curve), (b) $f_n = 0.95$ with f_e varying (dashed-dotted curve), (c) $f_n = 0.90$ with f_e varying (dotted curve) and (d) $f_n = f_e$ with both varying (solid line). From the confidence limits shown, it is apparent that the fits for the cases with unequal f_n and f_e are not statistically much better than the fit for case (d) with $f_n = f_e$, although lower minima are observed. In fig. 4 we show a comparison of the line shapes for cases (a) and (d) with the data. It is clear that in the case (a) the improvement in the fit is due to a deeper valley. From many line shapes examined in this work it was found that the LSS–Blaugrund slowing down theory predicts somewhat higher probability for small

TABLE 1

Calibration of the stopping power of Ni for Cu ions using DSA measurements from the ^{60}Ni(α, pγ)^{63}Cu reaction in conjunction with lifetimes from resonance fluorescence measurements.

Energy level (keV)	τ (fs) used for calibration	f_n[a]	f_e[a]	1660.2 keV in ^{61}Cu τ (fs)[b] deduced
669.7	310±30[11])	0.82±0.12	0.82±0.12	235±10[c]
1546.8	203±20[12])	0.86±0.09	0.86±0.09	
1546.8	203±20[13])	0.90	0.80±0.08	232±10
		0.95	0.73±0.07	231±10
		1.0	0.64±0.06	230±10

[a] Values at minimum chi-square.
[b] Values calculated for the 1660.2 keV transition in ^{61}Cu employing the stopping power factors indicated in columns 3 and 4. The errors indicated are only statistical.
[c] Calculated with $f_n = f_e = 0.84$.

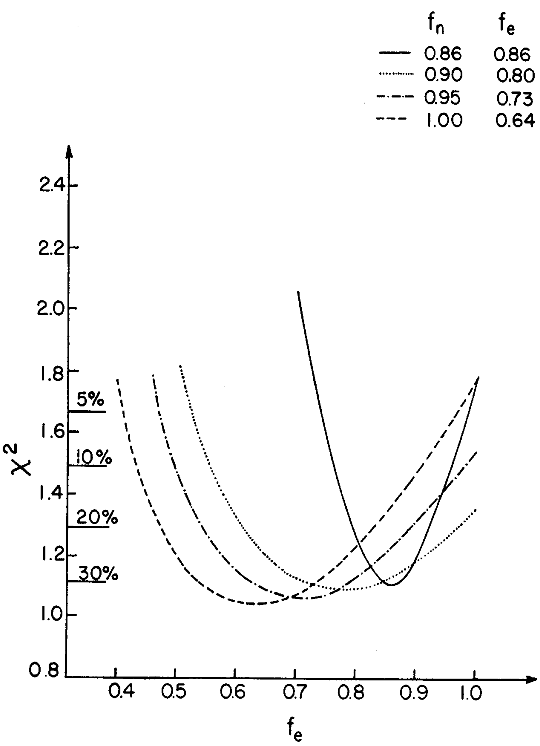

Fig. 3. Plots of the χ^2 for the fit of the calculated line shapes for the 1547 keV transition in ^{63}Cu with a known lifetime of 203 fs. The solid line corresponds to varying both the nuclear and electronic stopping powers by the factors f_n and f_e indicated relative to the LSS values. The dotted, dashed-dotted and dashed lines correspond to holding the f_n constant at the values indicated and varying f_e. The 5%, 10%, 20% and 30% confidence limits are also indicated.

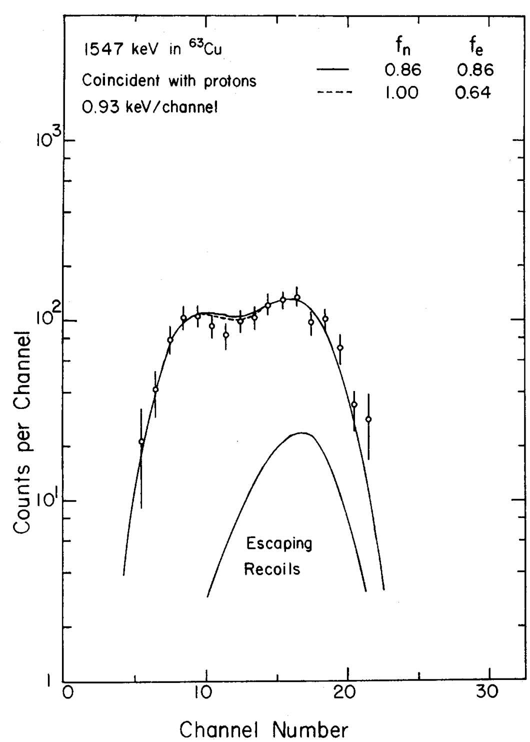

Fig. 4. Comparison with experiment of the calculated line shapes for the 1547 keV γ-ray in ^{63}Cu using the stopping power parameters indicated. The contribution to the spectrum due to the recoils that escape the target is displayed and it has been included in the line shapes shown. The target thickness in this case was 2.0 mg/cm^2.

TABLE 2

Application of the calibrated stopping power of Ni to previous DSA measurements with the $^{58}Ni(p, p'\gamma)$ reaction and comparison with independent results employing resonance fluorescence and electron scattering techniques.

Energy level (keV)	Mean lifetimes in fs		
	Values[a] with $f_e = f_n = 1.0$	Values with $f_e = f_n = 0.84$	From refs. 14 and 15
3038	57 ± 5	69.3 ± 6.0	75 ± 9[b]
3263	36 ± 2	43.7 ± 3.0	46 ± 5[b]
3593	48 ± 7	60.2 ± 8.9	68^{-19}_{+12}[c]

[a] Values obtained from ref. 13 including only the statistical error for $F(\tau)$.
[b] Weighted average from refs. 14 and 15.
[c] From ref. 14 only.

shifts than the data show. This rather minor difficulty may either be due to the nuclear stopping power itself being too low at low energies or it may be due to the average collision cosine[2]) which does not decrease rapidly enough with decreasing energy.

The effect of the different pairs of values for f_n and f_e from table 1 on the lifetimes extracted for the 1660.2 keV transition in ^{61}Cu from DSA coincidence data is summarized in the last column of table 1. It is clear that the lifetimes obtained are insensitive to the choice of pairs of values for the stopping power, as long as these values were obtained from a best fit to a "standard" peak. It may, therefore, be concluded that the choice of $f_e = f_n = 0.84 \pm 0.08$ is satisfactory for Cu ions slowing down in Ni.

In order to provide an independent check of this method for determining the stopping power of Ni, we reanalyzed the DSA measurements of Bertin et al.[13]) for the levels at 3038, 3263 and 3593 keV in ^{58}Ni excited via the $^{58}Ni(p, p'\gamma)$ reaction in coincidence experiments. The values for the lifetimes of these levels extracted by Bertin et al.[13]) using the (LSS) values for the stopping power are summarized in column 2 of table 2. These values are in good agreement with the independent measurements of Assimakopoulos et al.[3]) which also employed the DSA method with (LSS) values for the stopping power. By using the $F(\tau)$ values given by Bertin et al.[13]) and the adjusted stopping power with $f_e = f_n = 0.84$ we obtained the lifetimes shown in column 3 of table 2. These values are now in much better agreement with the weighted average (last column in table 2) of two sets of independent measurements employing resonance fluorescence[14]) and electron scattering[15]) techniques.

4.2. LINE SHAPES FROM COINCIDENCE AND SINGLES MEASUREMENTS

As it was discussed earlier, the line shapes obtained in coincidence experiments in reactions very close to threshold or in radiative capture reactions are independent of particle and γ-ray angular correlation effects. Singles experiments on the other hand, with reactions such as $(\alpha, p\gamma)$ or $(p, p'\gamma)$, yield shapes that depend on $d\sigma(\theta_R)/d\Omega$ and $W(\theta_R \phi_R \theta_d)$ as shown in eqs. (1) and (4). In fig. 5 we show a comparison with experiment of the line shape that gives the best fit (245 ± 24 fs) to the coincidence data for the 1904.1 keV transition in ^{61}Cu from the $^{58}Ni(\alpha, p\gamma)$ reaction at 10.0 MeV. Here the target used was 2.0 mg/cm^2 and the contribution to the shift from the recoils that escape from the target and decay in flight is substantial. In order to demonstrate the applicability of the method of sect. 2.1 in the calculation of line shapes, we show in fig. 6 the line shape for the 1904.1 keV γ-ray in ^{61}Cu from singles data

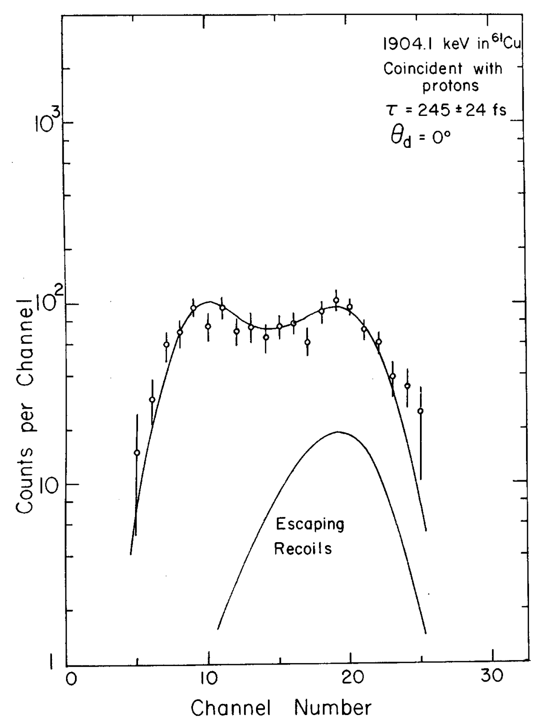

Fig. 5. Comparison of the calculated line shape for the 1904.1 keV γ-ray in ^{61}Cu with experimental data obtained at 0° to the beam in coincidence with protons detected in an annular Si detector. The lifetime that gave the best fit to these data was 245 ± 45 fs. It is seen that the experimental shape is reasonably well reproduced.

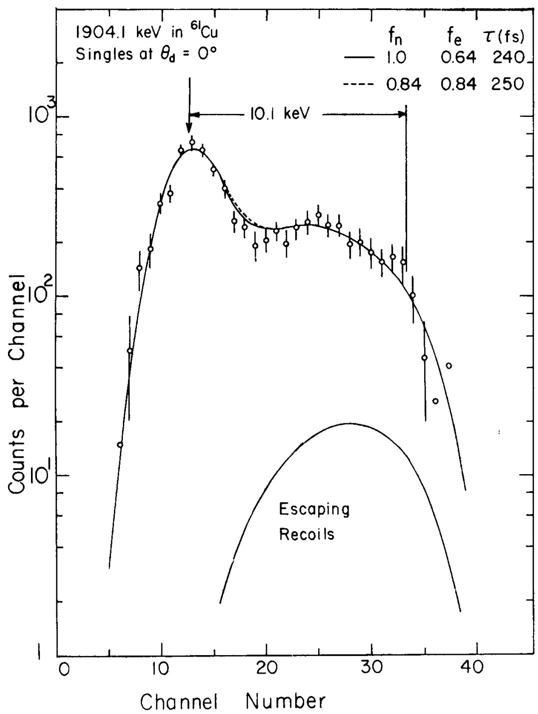

Fig. 6. Comparison with experiment of the line shape for the 1904.1 keV γ-ray in ^{61}Cu calculated with the stopping powers indicated. The data were obtained in a singles experiment at $\theta_d = 0°$. It is seen that the unequal parameters give a somewhat better fit to the data at lower Doppler shift values.

taken at 9.7 MeV with the detector at 0° to the beam direction. In this case $d\sigma(\theta_R)/d\Omega$ was obtained using eq. (6) with only the A_2 term included. The value of $A_2 = 0.365$ was employed and it was obtained from the differential cross section measurements at high particle resolution[8]). For the p–γ correlation the values of $\bar{A}_2 = 0.51$, $A_2^0 = 0.70$ and $\bar{A}_4 = A_4 = 0$ in eq. (10) were used. Furthermore, a fraction of 0.014 of nuclei in the 1904.1 keV state are populated via decay from the 3066 keV level in ^{61}Cu with a lifetime $\tau_2 = 57 \pm 9$ fs and this was included in the calculation of the line shape. The shape obtained fits the experimental data satisfactorily and gives a lifetime for the 1904.1 keV level in good agreement with the coincidence measurements.

Next, the dependence of the singles line-shape on the detection angle was evaluated via eqs. (1) and (4) and the results of two calculations are compared with experiment for $\theta_d = 30°$ and $\theta_d = 45°$. It is clear that the deviation from experiment progressively increases with increasing θ_d (compare figs. 6 and 7). Progressively the low shifts are overestimated. It is believed that in major part this is due to the ϕ_R dependence of the angular correlation functions of eq. (7).

In fact in some instances with $\theta_d = 90°$ a minimum at zero shift is observed[16]) which could not be reproduced if the ϕ_R dependence in eq. (7) is neglected. It is therefore suggested that the present approximation be used in line-shape calculations for cases where $\theta_d \leqslant 30°$ to the beam direction. As it will be shown below, however, this approximation does not affect the calculated $F(\tau_1, \tau_2, \ldots)$ values due to symmetry considerations.

In order to demonstrate the effect of uncertainties in the lifetimes due to uncertainties in $d\sigma(\theta_R)/d\Omega$ or $W(\theta_R \phi_R \theta_d)$ reflected on the calculated line shapes we have performed three calculations for the 1997.3 keV γ-ray in ^{61}Cu from a singles experiment. Firstly, the line shape was calculated for $\theta_d = 30°$ using a $d\sigma(\theta_R)/d\Omega$ distribution given by eq. (6) with $A_2 = 0.58$ and $A_4 = 0$ and a p–γ $W(\theta_R, \theta_d)$ distribution given by eqs. (7) and (10) with $A_2^0 = -0.5$, $\bar{A}_2 = -0.31$ and $A_4^0 = \bar{A}_4 = 0$. The solid curve in fig. 8 was obtained and this gave $\tau = 107 \pm 6$ fs. Secondly, the p–γ correlation was assumed isotropic but $A_2 = 0.58$, $A_4 = 0$ was used in the $d\sigma(\theta_R)/d\Omega$ distribution. The dashed curve was

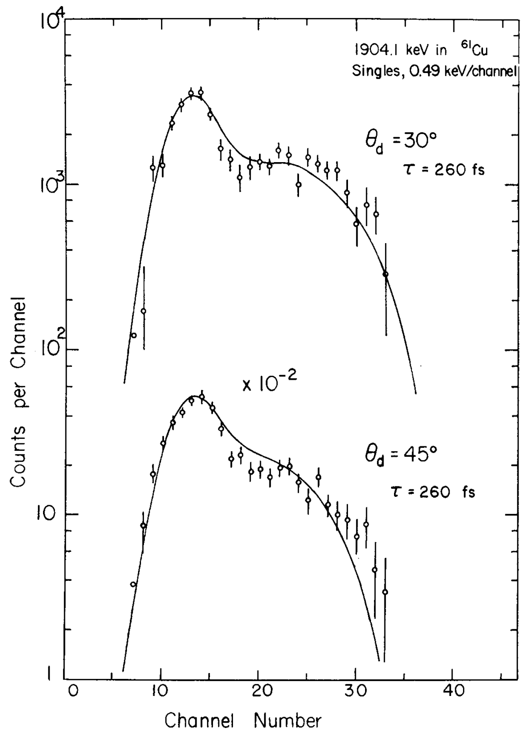

Fig. 7. Comparison of the line shapes from the 1904.1 keV γ-ray in ^{61}Cu with experimental data obtained in singles measurements at 30° and 45° to the beam. It is seen that the line shapes show progressively increasing deviation from experiment with increasing angle of observation. The low shifts are overestimated in the calculation and the high shifts are underestimated.

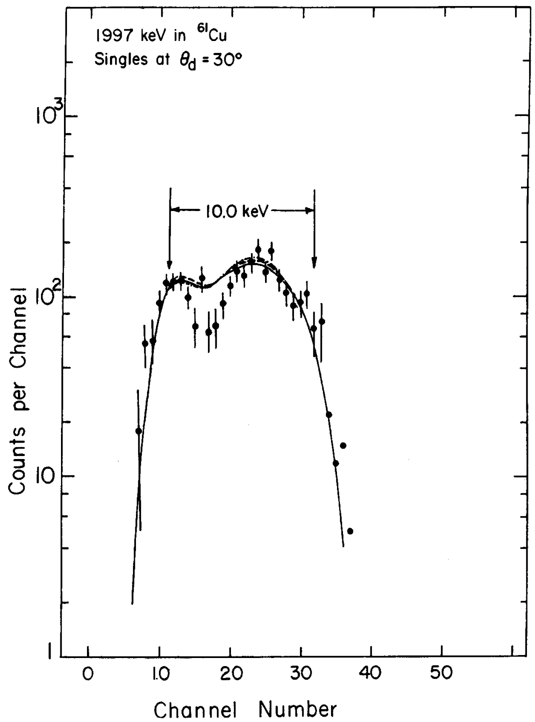

Fig. 8. Effect of the $d\sigma(\theta_R)/d\Omega$ distribution and the p–γ correlation on the calculated line shapes for the 1997.3 keV γ-ray in ^{61}Cu. For this highly shifted γ-ray the 30° shape was chosen where the agreement with experiment is rather poor, particularly at low shifts. The solid line includes both the $d\sigma(\theta_R)/d\Omega$ and the p–γ correlation in the analysis. The dashed dotted curve was obtained assuming an isotropic p–γ correlation but including an anisotropic $d\sigma(\theta_R)/d\Omega$ distribution. The dashed curve was obtained assuming both the $d\sigma(\theta_R)/d\Omega$ distribution and the p–γ correlation to be isotropic.

obtained with a $\tau = 102 \pm 6$ fs at minimum χ^2. Thirdly, the distribution $d\sigma(\theta_R)/d\Omega$ was also assumed to be isotropic in the CM system and this gave the dashed-dotted curve with $\tau = 104 \pm 6$ fs. From this comparison it is concluded that an error of $\leqslant 5\%$ in the lifetimes may be expected if these effects are neglected and isotropic distributions are assumed. Again the agreement of the calculated line shape with experiment for this highly shifted γ-ray at an angle of 30° to the beam is moderately good.

Finally it should be mentioned that the calculated line shape is affected significantly by the population of the observed state via other transitions from higher lying states. Two extreme cases are of interest. In the first case if a small fraction of the population is obtained via a long lived state, then the unshifted portion of the peak is increased. In the second case, a substantial fraction is formed via a state with comparable or shorter lifetime than the state observed. In this case the highly shifted portion of the peak is decreased both in energy and relative probability.

4.3. Centroid shifts from singles measurements

As it was mentioned in sect. 2.2 $F(\tau_1, \tau_2, \ldots)$ as defined by eq. (15) is expected to be to a good approximation independent of θ_d, so that eq. (14) holds. We have examined the applicability of eq. (14) to singles measurements from the ^{58}Ni(α, pγ) reaction and have found that for all cases considered a plot of E_γ as a function of $\cos\theta_d$ is to within experimental error linear. In fig. 9 we show the centroid shifts for the 1883.1, 1997.3 and 2.792.4 keV γ-rays measured for a wide range of angles (0°–110°) relative to the beam. The straight lines shown were obtained by least squares fits to the data. It is apparent that within experimental error no systematic deviation from a straight line dependence was observed.

5. Summary

From the results presented in this work it was

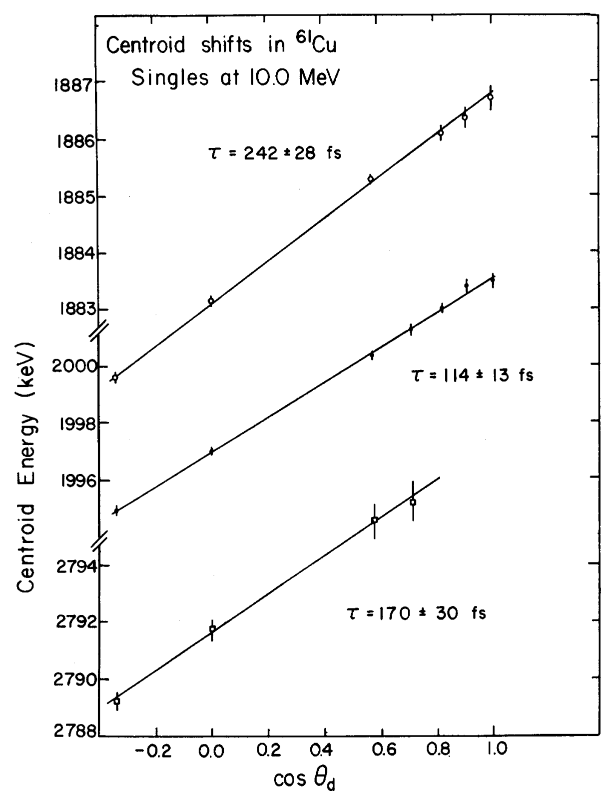

Fig. 9. Plots of the centroid energy for the 1883.1, 1997.3 and 2792.4 keV γ-rays from ^{61}Cu observed in singles experiments as a function of cos θ_d. A linear dependence for a wide range of angles is observed. The extracted lifetimes are also indicated.

demonstrated that the electronic and nuclear stopping powers can be effectively adjusted to reproduce the line shapes and centroid shifts for standard γ-rays of known lifetimes. These stopping powers in turn can be used via the DSA method to extract more accurate lifetimes. It was shown further that line shapes from both coincidence and singles measurements near and above threshold can be well reproduced by means of the "adjusted" stopping power theory, at least for detection angles $\leqslant 30°$ to the beam direction. This is possible for the singles results by some simple approximations for the outgoing particle correlation about the beam-direction and for the particle–gamma correlations. The effect of feeding from higher lying states was also incorporated in the calculation of both line shapes and centroid shifts. It was also shown, that even for thick targets the contribution to the shift due to recoils escaping the target and decaying in flight cannot be neglected. It is found that the best results are obtained when the line shapes can be determined experimentally particularly for angles between 0° and 30° to the beam. When the Doppler shifts are rather small, line shapes can not be obtained experimentally. In such cases and for singles measurements well above threshold it is recommended that the centroid shifts be measured as a function of angle of detection. From a plot of the centroid energies vs cos θ_d reliable values for $F(\tau_1, \tau_2, ...)$ can be obtained. In these cases the $F(\tau_1, \tau_2, ...)$ values should then be computed as a function of the lifetimes involved preferably at $\theta_d = 0°$.

We wish to express our thanks to Mr J. Hood and the personnel of the Washington University Cyclotron for their fine efforts throughout this series of experiments. The cooperation of the staff of the Washington University Computing Facilities is also appreciated. Two of us, E.J.H. and D.M.V.P., would also like to thank Mr C. Adams and the personnel of the University of Pennsylvania Tandem Van de Graaff Laboratory, for their cooperation in these experiments.

References

1) E. K. Warburton, J. W. Olness and A. R. Poletti, Phys. Rev. **160** (1967) 938.
2) A. E. Blaugrund, Nucl. Phys. **88** (1966) 501.
3) P. A. Assimakopoulos, T. Becker, C. Moazed and D. M. Van Patter, Nucl. Phys. **A180** (1972) 131.
4) W. M. Curnie, L. G. Earwaker and J. Martin, Nucl. Phys. **A135** (1969) 325.
5) M. Bister, A. Antilla, M. Piiparinen and M. Viitasula, Phys. Rev. **C3** (1971) 1972.
6) C. Broude, P. Engelstein, M. Popp and P. N. Tandon, Phys. Letters **39B** (1972) 185.
7) L. Lindhard, M. Scharff and H. E. Schiott, Mat. Fys. Medd. Dan. Vid. Selsk. **33**, no. 14 (1963).
8) E. J. Hoffman, D. G. Sarantites and N.-H. Lu, Nucl. Phys. **A173** (1971) 146.
9) F. Rauch, D. M. Van Patter and P. F. Hinrichsen, Nucl. Phys. **A124** (1969) 145.
10) M. E. Phelps, D. G. Sarantites and W. G. Winn, Nucl. Phys. **A149** (1970) 647.
11) T. Rothem, F. R. Metzger and C. P. Swann, Nucl. Phys. **22** (1961) 505.
12) C. P. Swann, private communication (1972).
13) M. C. Bertin, N. Benczer-Koller, G. G. Seaman and J. R. MacDonald, Phys. Rev. **183** (1969) 964.
14) F. R. Metzger, Nucl. Phys. **A158** (1970) 88.
15) M. A. Duguay, C. K. Bockelman, T. H. Curtis and R. A. Eisenstein, Phys. Rev. **163** (1967) 1259.
16) J. J. Kolata, R. Auble and A. Galonsky, Phys. Rev. **162** (1967) 957.